# STATISTICAL DECAY OF THE GIANT DIPOLE RESONANCE EXCITED BY COMPLETE FUSION REACTIONS AND OTHER SOURCES OF HIGH-ENERGY $\gamma$-RAYS IN HEAVY-ION COLLISIONS AT 4–11 MeV/u*

Marta Kicińska-Habior

Institute of Experimental Physics, Warsaw University
Hoża 69, 00–681 Warsaw, Poland

*(Received August 10, 1998)*

The $\gamma$-decay of the Giant Dipole Resonance, GDR, built on excited states of compound nuclei is discussed as a source of high-energy $\gamma$-ray emission in complete fusion reactions at projectile energies up to 5 MeV/u. Some results of the GDR studies are presented, also those measured at the Warsaw Cyclotron for the $^{12}C+^{58,64}Ni$ reactions at 47.5 MeV by using the new multi-detector system JANOSIK. The mechanism of heavy-ion collisions and sources of high-energy $\gamma$-ray radiation occurring at projectile energies of 6–11 MeV/u are also described. At these energies, besides statistical GDR decay, another process involving bremsstrahlung radiation becomes important. It is shown that in mass-asymmetric reactions, such as $^{12}C+^{24,26}Mg$ and $^{12}C+^{58,64}Ni$, the two types of $\gamma$-ray emission may be disentangled by the angular distribution measurement. The data when properly analyzed may give information on the GDR built on excited states as well as on the bremsstrahlung process.

PACS numbers: 24.30.Cz, 25.70.–z, 23.20.–g

## 1. Introduction

The intention of this talk is to present sources of high-energy ($E_\gamma$ = 10–50 MeV) $\gamma$-ray radiation emitted in heavy-ion collisions at projectile energies 4–11 MeV/u which are already or will be available soon at the Warsaw Cyclotron. It will also be shown what a study of this emission can teach us about a mechanism of the process and nuclei taking part in it. Character of the emitted radiation depends strongly on a projectile energy. Thus the

* Presented at the International Conference "Nuclear Physics Close to the Barrier", Warszawa, Poland, June 30–July 4, 1998.

presentation will be divided into two parts: for projectile energy up to 5 MeV/u and between 5 and 11 MeV/u. In the first part the properties of the Giant Dipole Resonance (GDR) built on the ground-state and excited states will be shortly reminded. Some previous results concerning studies of the evolution of the nuclear shape will be also shown. Finally, an experimental set-up built at the Warsaw Cyclotron [1] and new results [2] obtained here will be presented. In the second part, the results for reaction $^{12}$C+$^{24,26}$Mg, measured in Seattle [3], and new aspects in the data analysis [4] will be discussed and some preliminary results for $^{12}$C+$^{58,64}$Ni reaction [5] will be also shown.

## 2. Sources of high-energy $\gamma$-ray radiation in heavy-ion collisions at projectile energies up to 5 MeV/u

At projectile energies up to 5 MeV/u, which have been available at the Warsaw Cyclotron since 1995, the main source of high-energy $\gamma$-rays is the decay of the Giant Dipole Resonance excited in hot, rotating compound nuclei formed by fusion reactions. Gamma-ray spectrum measured in such process has characteristic shape which can be divided into four parts corresponding to different paths of the decay. Photons with the highest energy are emitted from the initial compound nucleus in competition with evaporation of the first particle and from daughter nuclei after emission of one or two particles. These photons arise from the decay of the GDR built in the initial compound nucleus and in the daughter nuclei with lower mass and lower excitation energy. Lower-energy $\gamma$-rays are emitted during the next steps of the decay from daughter nuclei already cooled down by particle evaporation. The lowest energy $\gamma$-rays, E2 photons, are emitted when the nucleus is left with an excitation energy close to the yrast line, and a substantial angular momentum. Thus, analyzing the high-energy bump in the $\gamma$-ray spectrum, we are able to get an information concerning high-frequency collective vibrations of protons against neutrons, called Giant Dipole Resonance, in hot rotating nucleus.

### *2.1. GDR in the ground-state nuclei*

At zero temperature these oscillations, occurring in all nuclei, have a resonance character with the resonance energy $E_{\mathrm{GDR}}$ inversely proportional to the length of the nuclear axis in the direction of oscillations. As a consequence, for spherical nuclei, the observed GDR strength function is described by a single resonance, whereas for deformed axially symmetric nuclei — by a double resonance curve, characteristic for a given shape of the nucleus. Quadrupole deformation $\beta$ of the nucleus can be inferred from the energy splitting of the resonance. A single resonance shape is well reproduced by a

Lorentzian function, with parameters: $S$, $E_{\rm GDR}$, and $\Gamma$. The GDR parameters for ground-state nuclei extracted from many experiments have been collected by Gaardhoje [6] (see Fig. 8 in [6]). The strength $S$, describing collectivity of the vibrations, is close to 1 in units of the energy weighted sum rule, in agreement with theoretical expectations. The resonance energy, $E_{\rm GDR}$, related to the magnitude of the restoring force, decreases gradually with increasing mass number A. The resonance width $\Gamma$ at zero temperature varies in the range of 4–8 MeV. It can be explained by the coupling of the GDR to $2p--2h$ states and more complicated states which produces the intrinsic GDR width. The lowest widths are observed for magic nuclei which is the effect of shell-effects affecting the density of 2p–2h states. As it was already shown, in case of deformed nuclei an additional splitting occurs, enlarging the width.

### *2.2. GDR built on excited states*

In heavy-ion collisions nuclei at finite temperature and high angular momenta are formed. The GDR, according to the Brink hypothesis [7], can be built on any state with an excitation energy $E_x$ and spin $I$. Thus, in order to explain behavior of the GDR, the effect of the temperature and the rotation has to be taken into account. The GDR parameters extracted for many nuclei at excitation energy of 30–100 MeV have been also collected in Ref. [6]. The excitation energy dependence of the GDR parameters which includes temperature and spin dependence is shown for one particular nucleus $^{63}$Cu [8] in Fig. 1. The GDR strength, and the centroid energy, are not affected by the temperature and spin. The widths are in general larger than in the ground-state and increase with increasing temperature and spin. The GDR parameters extracted from the experimental $\gamma$-ray spectra by fitting statistical model calculations in the range of the GDR bump are averaged over the decay steps. It is thus important to present the GDR parameters as a function of an average final excitation energy and an average spin, which may differ substantially from the initial values.

In order to explain behavior of the GDR width several effects are taken into account with temperature and spin increasing. With increasing temperature shell-effects are washed-out and a nucleus behaves as a rotating liquid drop changing gradually deformation with increasing angular momentum. At finite temperature the nuclear shape is not "frozen" but can fluctuate around the equilibrium deformation. Thus, the coupling of the GDR vibrations to the low frequency but large amplitude fluctuations of the nuclear surface has much more complicated result [9] than at $T = 0$.

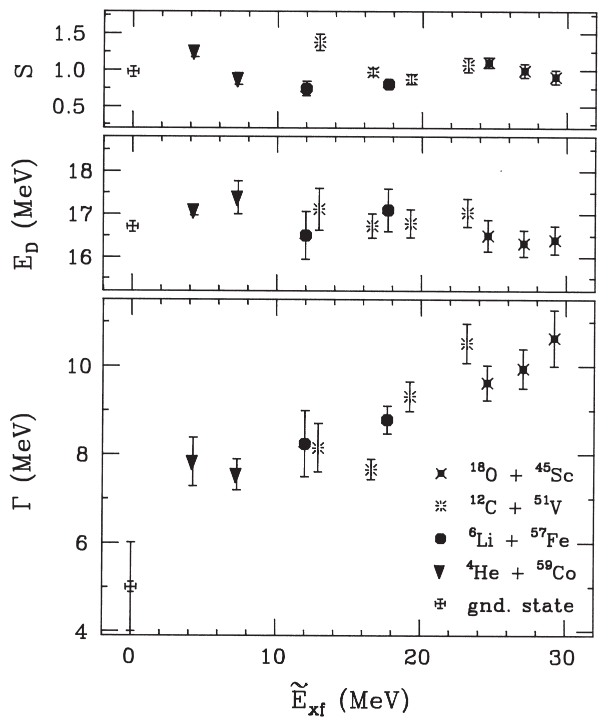


Fig. 1. GDR parameters for $^{63}$Cu nuclei as a function of final excitation energy, from [8].

Probability of a given shape is described by the Boltzmann factor. GDR can be built in a nucleus in each probable shape. Thus, the observed GDR strength function is a result of averaging of the GDR vibrations over the whole ensemble of deformed shapes. As the temperature increases the probability of shapes far from equilibrium deformation gets larger. The resulting spread in resonance energies will increase, giving rise to a larger width. As the angular momentum increases the Coriolis and centrifugal forces tend to increase the deformation of the nucleus, which also results in an increase of the total width. The sensitivity of the GDR width to spin is larger for lighter nuclei because of their smaller moments of inertia. In order to extract from the experimental GDR data an information about the mean as well as equilibrium deformation of the hot, rotating nucleus the thermal shape and orientation fluctuation theory has to be applied [9]. It was shown recently by Kusnezov, Alhassid, and Snover [10] that the GDR width in hot rotating nuclei, which is a function of temperature $T$ and spin $I$, may be described in the framework of the thermal fluctuation theory by one global phenomenological function in a broad range of nuclear masses. Thus, at high spin the effect of rotational energy dominates and the width depends on $\xi = I/A^{5/6}$, after taking into account shape fluctuations. Additional information about the nuclear shape is contained in the angular distribution of $\gamma$-rays emitted during the GDR decay. The measured angular distributions transformed to the nucleus-nucleus CM frame can be presented as a sum of Legendre polynomials which in case of the statistical emission is limited to: $d^2\sigma(E_\gamma, \theta_{\rm CM})/d\Omega dE_\gamma = A_0(E_\gamma) \cdot [1 + a_2(E_\gamma) \cdot P_2(\cos\theta_{\rm CM})]$. For a deformed nucleus a characteristic dispersion shape of $a_2$ versus $E_\gamma$ is expected to occur, centered about the mean GDR energy, while for a spherical nucleus $a_2 = 0$. The observed $a_2$ coefficient is also averaged over the ensemble of possible shapes. Thermal fluctuation theory explains successfully both the observed cross section and the angular anisotropy [11].

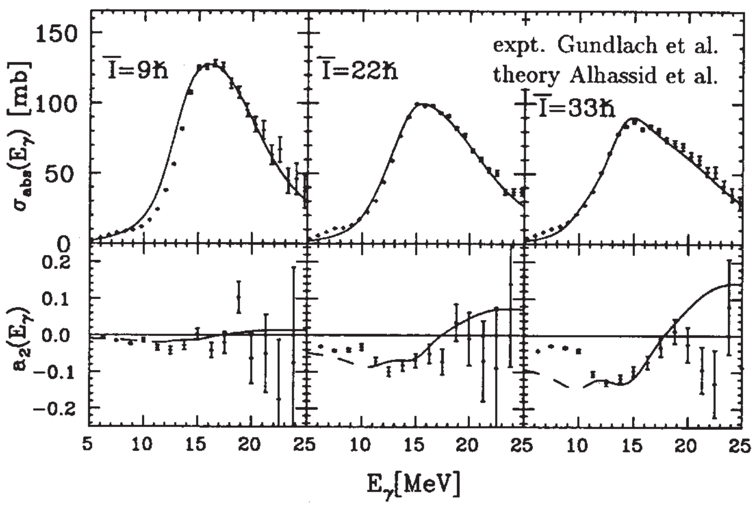


Fig. 2. GDR strength functions and angular distribution coefficients $a_2$ for $^{90}$Zr and $^{92}$Mo, from [12].

As an example of the nuclear shape evolution studies with an increasing temperature and spin, the evolution of the GDR strength function for a nucleus spherical in the ground-state: $^{90}$Zr and $^{92}$Mo studied at an average spin and temperature in the range of $I$ = 9–33 $\hbar$ and $T$ = 1.6–2 MeV [12] is shown in Fig. 2. From the measured strength functions and angular distributions compared with the thermal shape fluctuation theory [13], the shape evolution from spherical to oblate with $\beta_{eq} = 0.02 - 0.16$, was inferred. Another case illustrates the shape evolution of $^{45}$Sc [14], a light nucleus in which at very high rotation the nucleus can survive fission. It is predicted in the liquid drop model that at very high rotation the equilibrium shape should undergo a shape transition from oblate to triaxial, approximately prolate, with a superdeformed major-to-minor axis ratio of 2:1 or greater. As it is shown in Fig. 3, thermal shape and orientation fluctuation calculations reproduce well the experimental GDR strength functions for $^{45}$Sc nuclei at an average spin $I = 13$–$23.5\ \hbar$. However when the oblate-to-triaxial shape transition has been removed, the calculated strength functions do not agree with experiment at high spins.

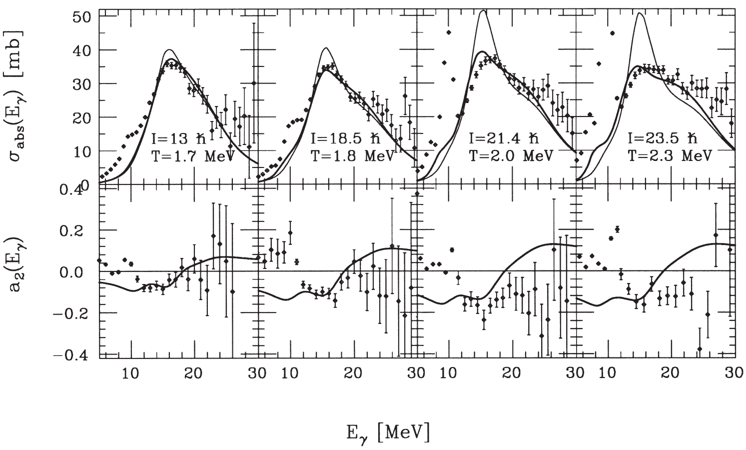


Fig. 3. GDR strength functions and angular distribution coefficients $a_2$ for $^{45}$Sc, from [14]. Heavy solid curves — fluctuation calculations with the phase transition; light curves — with phase transition removed.

This confirms that the observed broadening of the GDR strength function is mostly due to the spin-induced deformations. The calculated $a_2(E_\gamma)$ at higher spins agree with the data only on the low energy side of the resonance. At $E_\gamma$ energies above the GDR centroid discrepancies are observed for high projectile energies. This effect has been also seen in the coincidence experiments for $^{32}$S+$^{27}$Al [15] (Seattle) as well as $^{18}$O+$^{28}$Si [16] (Copenhagen). It is still a puzzle. The data shown in Fig. 3 were collected in a nearly mass-symmetric reaction $^{18}$O+$^{27}$Al, at projectile energies $E_p/A =$ 2.5–6 MeV/u. The bremsstrahlung emission was suggested as a possible source of the $a_2$ coefficient discrepancies at the highest projectile energy.

### *2.3. First GDR experiments at the Warsaw Cyclotron*

In order to study shape evolution in medium mass-nuclei and to have a possibility to disentangle the statistical GDR decay and the bremsstrahlung radiation, the project for mass-asymmetric $^{12}$C $+^{58,64}$Ni reactions has been started [5], producing $^{70}$Se and $^{76}$Se nuclei at several excitation energies and spins. The low energy structure for $^{70}$Se resembles the pattern characteristic for vibrational nuclei [17], suggesting spherical shape. However, $^{76}$Se is clearly showing the deformation in the ground-state [18] which is also seen in the GDR strength function [19]. Thus, with increasing spin, $^{70}$Se nuclei are expected to become oblate, whereas $^{76}$Se, being prolate, should also change its deformation towards oblate.

The project was proposed for the Warsaw Cyclotron. Thus, as a first goal an experimental set-up suitable to measure high-energy $\gamma$-rays was built at the Warsaw Cyclotron beam-line [1]. In this multi-detector system JANOSIK high-energy $\gamma$-rays are detected in a 25 cm $\times$ 29 cm NaI(Tl) crystal which is surrounded by an active plastic shield 10 cm thick, made by BICRON, passive $^{6}$LiH shield and a low activity 10 cm thick lead shield. Cosmic rejection efficiency obtained with those shields is not worse than 98%. The multiplicity of low-energy $\gamma$-rays is measured by the multiplicity filter, which consists of 32 small scintillator detectors. The $n$4-4$\gamma$ discrimination achieved by the standard time of flight technique with the time resolution of 4.5 ns at a 83 cm distance between the crystal face and the target allows a very good separation of the events induced by $\gamma$-rays produced in the target and by neutrons.

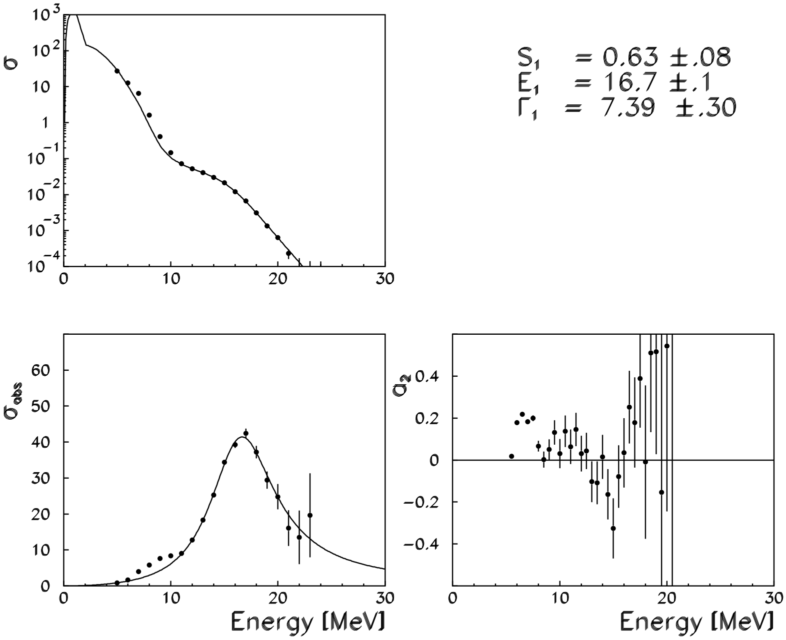


Fig. 4. Gamma-ray spectrum, GDR strength function, angular distribution coefficient $a_2$ and GDR parameters extracted from fit for the reaction $^{12}$C+$^{58}$Ni at $E_p$= 47.5 MeV; lines — CASCADE fit; [2].

Gamma-ray spectra from the decay of $^{70}$Se and $^{76}$Se produced by the $^{12}$C+$^{58,64}$Ni reactions at projectile energy of 47.5 MeV have been measured at three angles of 60°, 90° and 120° [2]. In order to get correct angular distributions the data normalization at different angles has been additionally checked by comparing to the spectrum measured with the Ge(Li) placed at the constant angle with respect to the beam axis. Compound nuclei of $^{70}$Se and $^{76}$Se have been produced at initial excitation energy of $E_x = 39.0$ and 45.5 MeV, respectively. Gamma-ray spectra have been collected with a good-enough statistics to allow for least-square fitting of statistical model calculations. The GDR parameters and strength functions were extracted from the fit, and the latter can be compared in a linear scale with the fitted Lorentzian shapes. It can be concluded from the fitted spectra that in case of $^{70}$Se where the fit with single Lorentzian is possible (see Fig. 4), the observed shape of the nucleus at an average temperature of $T = 1.4$ MeV, and an average spin of $I = 13\ \hbar$ is still spherical or close. For $^{76}$Se, the measured $\gamma$-ray spectrum can be fitted only with double Lorentzian GDR strength function (see Fig. 5) and the ratio of the component strength $S_2 : S_1 = 2.1 \pm 1.7$ does not disagree with the prolate shape.

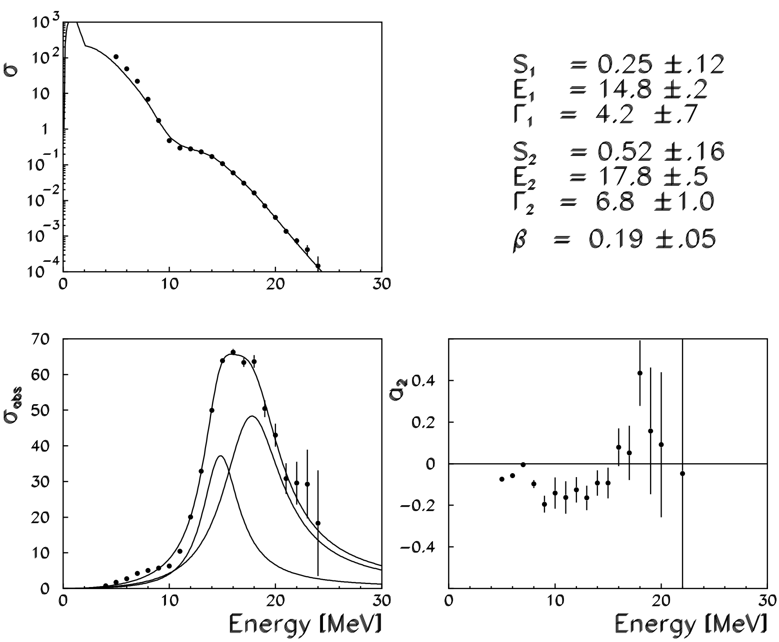


Fig. 5. Gamma-ray spectrum, GDR strength function, angular distribution coefficient $a_2$ and GDR parameters extracted from fit for the reaction $^{12}$C+$^{64}$Ni at $E_p$= 47.5 MeV; lines — CASCADE fit; [2].

The deformation coefficient inferred from split GDR energies is $\beta = 0.19 \pm .05$. The angular distributions have been fitted after transforming to the nucleus-nucleus CM frame by the sum of Legendre polynomials:

$$d^2\sigma(E_\gamma, \theta_{\rm CM})/d\Omega dE_\gamma$$
$$= A_0(E_\gamma)[1 + a_1(E_\gamma)P_1(\cos\theta_{CM}) + a_2(E_\gamma)P_2(\cos\theta_{CM})]\,.$$

The $a_1$ coefficient should be zero for statistical decay and it is used at this low projectile energy mainly to check the quality of the data. In a $^{76}$Se case the $a_2$ coefficient is clearly showing the dispersion shape (Fig. 5) which proves the deformation of the $^{76}$Se nuclei at the excitation energy and spin studied in agreement with the results obtained from the spectrum fits. The fact that the deformation coefficient extracted from the energy splitting of the GDR in excited nucleus is close to the value $\beta \approx 0.22$, obtained in a similar way from the GDR ground-state data, suggests that at this low excitation the nucleus maintains the shape which is probably the result of the shell structure. The $a_2$ coefficient for $^{70}$Se nuclei has different character shown in Fig. 4. It has smaller dispersion below the GDR centroid energy, but above the resonance it is still increasing. This data may suggest small deformation but such statement has much less confidence. The results presented in Fig. 4 for $^{70}$Se and in Fig. 5 for $^{76}$Se have been measured at the Warsaw Cyclotron beam from the PIG source. Substantial improvement of the quality of the data as well as the statistics is expected in future experiments with the ECR source.

## 3. Sources of high-energy $\gamma$-ray radiation in heavy-ion collisions at projectile energies in the range of 6–11 MeV/u

In order to continue the project for shape evolution studies of $^{70,76}$Se nuclei at projectile energies higher than those possible to reach in 1997 at the Warsaw Cyclotron [2], the $^{12}$C+$^{58,64}$Ni reactions have been studied at the University of Washington Nuclear Physics Laboratory using the Superconducting Linear Accelerator. High-energy $\gamma$-ray spectra at five angles (40°, 55°, 90°, 125° and 140°) have been measured for both targets with a new triple NaI-spectrometer set-up at three beam energies: 5.4, 8.3 and 11.2 MeV/u [5]. The experimental set-up presently available in Seattle consists of a previous Seattle detector of 25.4 cm $\times$ 32.1 cm, an Ohio State University detector of 29.2 cm $\times$ 38.1 cm, and an University of Illinois detector of 25.4 cm $\times$ 27.9 cm. To suppress background $\gamma$-rays and cosmic radiation each of them is surrounded by its own active plastic shield and a passive lead shield. A $^6$LiH shield absorbing thermal neutrons is also present, except in the Ohio State University detector, which is easily visible in comparing time spectra for all spectrometers. All three NaI-spectrometers are placed on carts, which can be moved on the special platform by floating on four air-pads. The set-up allows for a simultaneous measurement of high-energy $\gamma$-rays at three angles by rotating detectors around the target axis. In order to control and stabilize the gain of the detectors a LED pulser is used. The multiplicity of low energy $\gamma$-rays is measured by the multiplicity filter consisting of 22 small NaI detectors. The $n$-$\gamma$ discrimination achieved by the standard time of flight technique allowed for a very good separation of the events induced by $\gamma$-rays produced in the target and by the neutrons. During the experiment the $p$+$^{11}$B reaction at 7.25 MeV and 16 MeV proton beam energies has been also measured in order to get an information concerning an energy calibration and a response function for each NaI-spectrometer. Measured data are resently being analyzed.

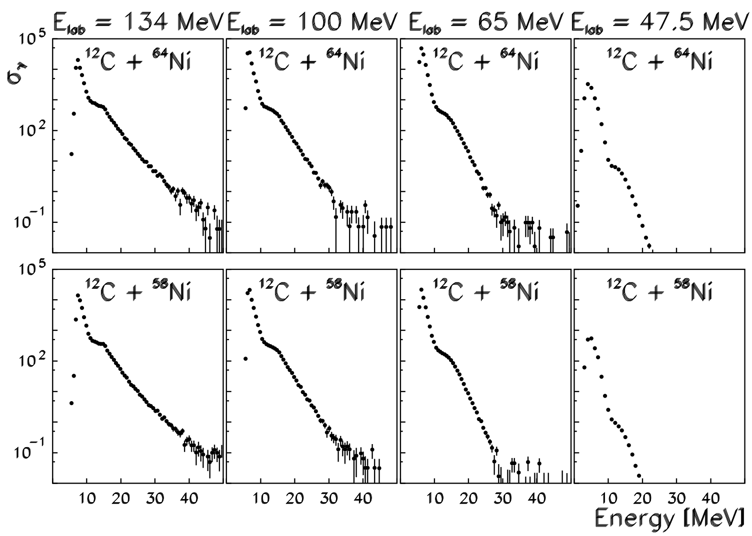


Fig. 6. Gamma-ray spectra for the reaction $^{12}$C+$^{58,64}$Ni at E$_p/A$= 5.4-11 MeV/u [5], (preliminary data), and at $E_p$ = 47.5 MeV [2].

Some spectra of high-energy $\gamma$-rays measured with Seattle detector placed at 90° with respect to the beam axis and obtained after preliminary analysis are shown in Fig. 6. Besides the characteristic strong low energy component a prolonged nearly exponential component increasing with projectile energy is clearly seen at $\gamma$-ray energies above 20 MeV. At these higher projectile energies statistical GDR decay is not the only source of high-energy photons. The mechanism of the collision is more complicated than just a complete fusion. I will discuss it on an example of $^{12}$C+$^{24,26}$Mg reactions data measured also in Seattle at projectile energies of 6, 8.6 and 11.2 MeV/u [3], for which some new aspects of the analysis have been recently included

[4]. In Fig. 7 the angular coefficients $A_0(E_\gamma)$, $a_1(E_\gamma)$ and $a_2(E_\gamma)$ extracted in the nucleus-nucleus CM frame from the data by fitting Legendre polynomials are presented for magnesium targets [3]. The spectra show a nearly exponential shape at energies above 20 MeV with an inverse slope increasing with bombarding energy. The $a_1(E_\gamma)$ coefficients in the nucleus-nucleus CM frame are positive and the asymmetry of the angular distributions increases with the projectile energy increasing, which suggests an existence of a non-statistical $\gamma$-ray emission. The $a_2(E_\gamma)$ coefficients have large negative values, presumably indicating very large deformation of the compound nucleus in which GDR is built.

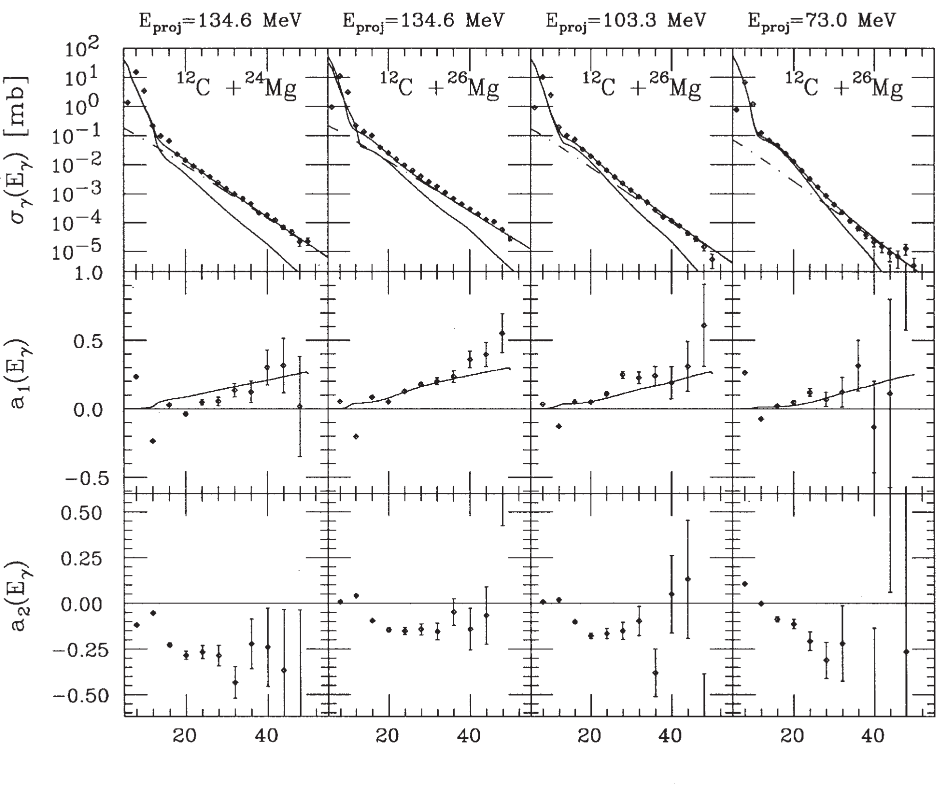


Fig. 7. Gamma-ray spectra and angular distribution coefficients for the reaction $^{12}$C+$^{24,26}$Mg at E$_p/A$= 6-11 MeV/u [3]; lines — CASIBRFIT fits with $E_0$ = const.

It is well known that at projectile energies studied two main mechanisms of the high-energy $\gamma$-ray emission in heavy-ion collision take place: statistical emission with the GDR decay and bremsstrahlung emission in the initial stages of the collision process. At projectile energies above 5 MeV/u statistical GDR decay may follow formation of the compound nucleus by the complete fusion as well as by an incomplete fusion reaction. In case of incomplete fusion of $^{12}$C projectile the transfers of $^{8}$Be and $^{4}$He to the compound nucleus are most probable. Also pre-equilibrium nucleon emission may take place before the compound nucleus thermalization.

Already at projectile energies below 5 MeV/u the extracted GDR parameters correspond to the average nucleus. When an incomplete fusion starts to be important, an average compound nucleus has lower mass as well as lower excitation energy. In the analysis [4] presented here of $^{12}$C+$^{24,26}$Mg data, the effort was made to account for all these processes and estimate their influence on GDR. I would also like to show that from the simultaneous analysis of $\gamma$-ray spectra and angular distributions one is able to differentiate between statistical decay and nucleon-nucleon bremsstrahlung, assuming that the collision is mass-asymmetric. Experiments discussed here have an inclusive character, thus an information concerning mechanisms additional to the statistical GDR decay has to be based on some other experimental results and/or theoretical estimates. The single but strong experimental constraint included in the analyzed data is the $a_1(E_\gamma)$ dependence on $E_\gamma$ energy.

An importance of the incomplete fusion process was estimated on the basis of $^{12}$C+$^{51}$V [20] and $^{16}$O+$^{27}$Al [21] reactions studied in the range of bombarding energies discussed here. Pre-equilibrium emission estimates are based on $^{12}$C+$^{103}$Rh [22] and $^{18}$O+$^{100}$Mo [23] experiments as well as on theoretical calculations with Fermi jet code [24]. As a result, the amount of incomplete fusion was estimated to be of the order of 20–30% for 6–11 MeV/u, the average initial compound nucleus formed by complete and incomplete fusion was found to be $^{36}$Cl, and its initial excitation energy — to be lower by 12–20%, compared with $^{38}$Ar formed by complete fusion. Bremsstrahlung process may be estimated on the basis of experiments at higher projectile energies where this process is dominating as well as on the basis of BUU (Boltzmann–Uehling–Uhlenbeck) nuclear transport equation [25].

BUU calculations have been performed for $^{12}$C+$^{24,26}$Mg for different impact parameters $b$ = 0, 2, 3.9, 5.5, 6.25 and 7 fm [4] with the code supported by Wolf [25]. The BUU cross-section calculated as $\sigma_{\rm BUU}(E_\gamma) = 2\pi\int_0^{b_{max}} P(b)\, b\, db$, where $P(b)$ is the $\gamma$-ray emission probability, was also fitted with an exponential formula $\sigma_{\rm BUU}(E_\gamma) = \sigma_0 \exp(-E_\gamma/E_0)$ in order to extract an inverse slope parameter $E_0$. It was found that $\sigma_{\rm BUU}(E_\gamma)$ is not really reproduced with a single $E_0$ value in the whole range of $E_\gamma$ = 10–50 MeV. The $E_0$ value extracted for different energy intervals changes by about 10%. This behavior can be compared with the experimental results at higher projectile energies found for Kr + Ni and Ta + Au reactions at

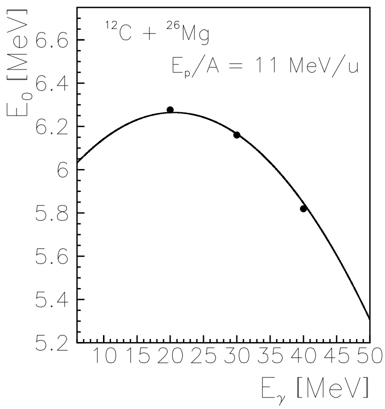


Fig. 8

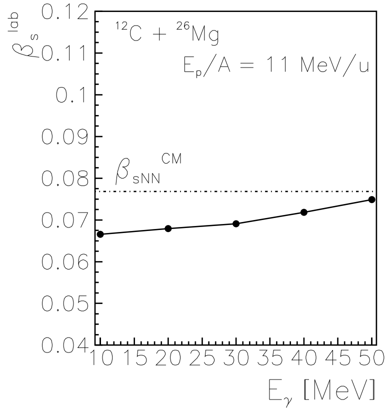


Fig. 9

Fig. 8. Fig. 8. Energy dependence of the inverse slope parameter $E_0(E_\gamma)$; (see text).

Fig. 9. Energy dependence of the mean source velocity calculated with BUU, averaged over impact parameter.

60 and 40 MeV/u, respectively (see Fig. 20 in [26]). Thus, simple parabolic energy dependence $E_0(E_\gamma) = E_0^0(1 + 0.0078 \cdot E_\gamma - 0.00019 \cdot E_\gamma^2)$ shown as a line in Fig. 8 has been proposed [4] to reproduce changes of $E_0(E_\gamma)$ value found from BUU calculations for $^{12}$C+$^{24,26}$Mg (points in Fig. 8) as well as an experimental trend at higher projectile energies. The $E_0^0$ was treated as a variable parameter in CASIBRFIT calculations discussed further. The mean velocity of the emitting source was also calculated with BUU. It depends on the photon energy and on the impact parameter $b$. With increasing $E_\gamma$, the value of $\beta_s$, averaged over impact parameter, approaches the value of the nucleon-nucleon CM velocity $\beta_{sNN}^{\mathrm{CM}}$ (see Fig. 9).

Statistical decay have been calculated according to the CASCADE code with the isospin correctly included, level density in the Reisdorf approach, and the spin-dependent moment of inertia. Though the measured $a_2(E_\gamma)$ coefficients suggested large deformations at higher spins, statistical model calculations have been done in all cases with a single Lorentzian GDR strength function. Calculations were done assuming a possibility of incomplete fusion with lowered initial excitation energy of the $^{36}$Cl compound nucleus. In order to take advantage of the $a_1(E_\gamma)$ dependence on $E_\gamma$ energy, which is a strong experimental constraint in the fitting procedure done with code CASIBRFIT [27], the coefficients $A_0(E_\gamma)$ and $a_1(E_\gamma)$ have been fitted simultaneously. It was assumed that in the nucleon-nucleon CM frame the bremsstrahlung emission has an isotropic angular distribution but the dipole

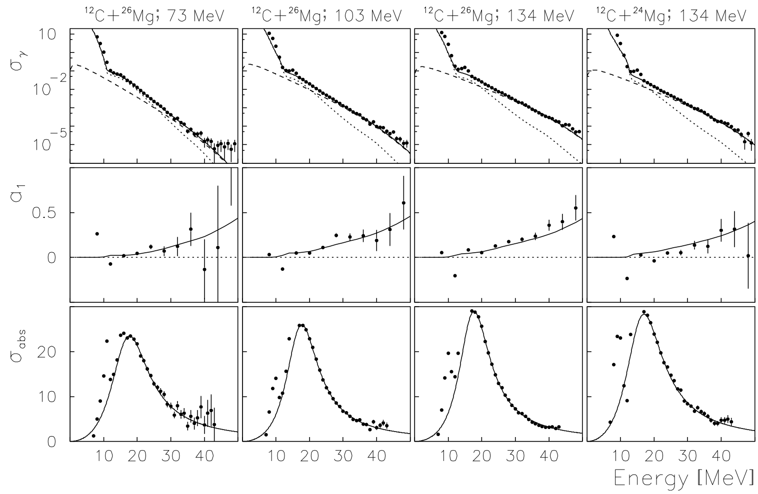


Fig. 10. Gamma-ray spectra, angular distribution coefficients $a_1$ and GDR strength functions for the reaction $^{12}$C+$^{24,26}$Mg at $E_p/A=$ 6-11 MeV/u; lines — CASIBRFIT fits with $E_0 = E_0(E_\gamma)$.

component suggested at higher projectile energies [26] was also tested and gave a very small change. According to the results of the BUU calculations in the new version of the CASIBRFIT code, a possibility to use $E_0 = E_0(E_\gamma)$ and $\beta_s = \beta_s(E_\gamma)$ was initiated. The fits were done with 5 variable parameters: $S$, $E_{\rm GDR}$, $\Gamma$, $\sigma_0$, $E_0$ (or $E_0^0$), for different options with $E_0 =$ const, $\beta_s =$ const, $E_0 = E_0(E_\gamma)$ and $\beta_s = \beta_s(E_\gamma)$. In order to reproduce the $a_1(E_\gamma)$ coefficient data, an $E_\gamma$ dependence of $E_0$ shown in Fig. 8 had to be included. The fits with only the energy dependent $\beta_s$ describing the BUU trend (Fig. 9) failed to reproduce $a_1(E_\gamma)$.

Fitted high-energy $\gamma$-ray spectra and $a_1(E_\gamma)$ coefficients for the best fits obtained with $E_0 = E_0(E_\gamma)$ and $\beta_s =$ const as well as appropriate GDR strength functions are shown in Fig. 10 together with the data. It can be seen that the used energy dependence of $E_0 = E_0(E_\gamma)$ gives lower bremsstrahlung cross-section at low $E_\gamma$ energies than in case of $E_0 =$ const (compare with Fig. 7). The GDR parameters extracted from the best fits as a function of the average final excitation energy $E_{xf}$ and the bremsstrahlung parameters as a function of the $v/c$ ratio are shown in Fig. 11 and 12, respectively. It can be seen that the GDR excited in $^{12}$C+$^{24,26}$Mg reaction has full strength and has a broad width nearly constant with excitation energy which corresponds to nearly constant average final spin. The bremsstrahlung parameters $\langle E_0\rangle =$ $E_0$ ($E_\gamma$ = 30 MeV) extracted from the fits are in agreement with values extrapolated from the Cassing systematics [25,26].

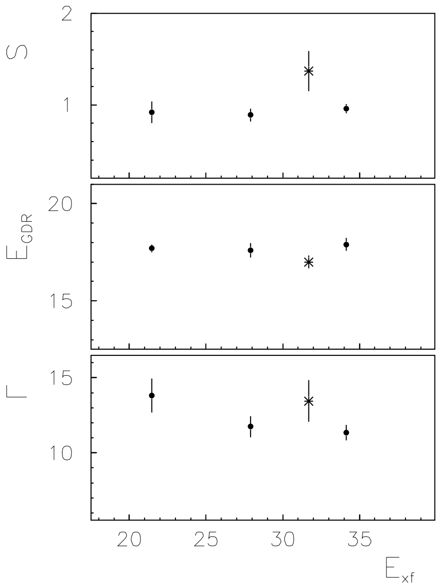


Fig.11

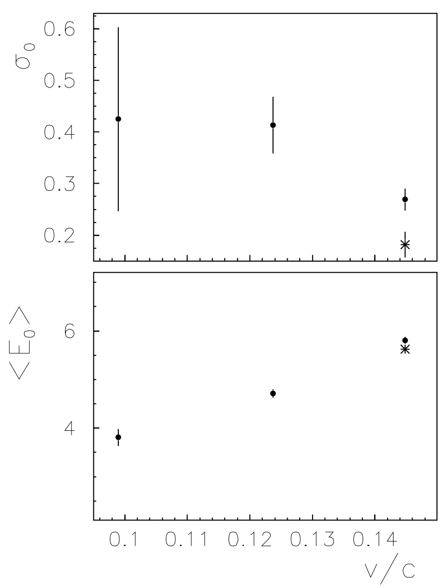


Fig. 12

Fig. 11. GDR parameters extracted from the fits for the reaction $^{12}$C+$^{24,26}$Mg; star — $^{24}$Mg, circles — $^{26}$Mg.

Fig. 12. Bremsstrahlung parameters extracted from the fits for the reaction $^{12}$C+$^{24,26}$Mg; star — $^{24}$Mg, circles — $^{26}$Mg.

## 4. Conclusions

It was shown that high-energy $\gamma$-rays from heavy-ion collisions at 6–11 MeV/u can be used as a source of information about the GDR at high excitation when experimental data are consistently analyzed. By reproducing simultaneously the $\gamma$-ray spectra and the $a_1(E_\gamma)$ coefficients it is possible to obtain also an information about the bremsstrahlung process. Analyzed data for $^{12}$C+$^{24,26}$Mg reaction as well as preliminary data for $^{12}$C+$^{58,64}$Ni reaction suggest that the inverse slope parameter $E_0$ depends on $\gamma$-ray energy which may correspond to its dependence on impact parameter. There are some plans to continue studies of high-energy $\gamma$-ray emission at the Warsaw Cyclotron in more exclusive experiments.

This work was partly supported by the Polish State Committee for Scientific Research (KBN Grant No. 2 P302 071 07).

## REFERENCES


[1] M. Kicińska-Habior, Z. Trznadel, M. Kisieliński, M. Augsburg, D. Chmielewska, J. Dworski, A. Kordyasz, M. Kowalczyk, J. Kownacki, A. Krzyczkowska, J. Kwieciński, A. Maj, T. Matulewicz, J. Romanowski, Z. Sujkowski, Z. Żelazny, *Acta Phys. Pol.* **B28**, 219 (1997).

[2] Z. Trznadel, M. Kicińska-Habior, M. Kisieliński, D. Chmielewska, P. Cichocki, B. Fornal, W. Jackowski, M. Kmiecik, M. Kowalczyk, J. Kownacki, A. Maj, T. Matulewicz, J. Styczeń, Z. Sujkowski, to be published.

[3] M. Kicińska-Habior, K.A. Snover, A. Maj, Z. Drebi, D. Ye, M. Kelly, *Acta Phys. Pol.* **B26**, 439 (1995).

[4] M. Kicińska-Habior, Z. Trznadel, A. Maj, M. Kelly, J.P.S. van Schagen, K.A. Snover, *Proceedings of the Topical Conference on Giant Resonances, Varenna, May 11-16, 1998*, to be published in *Nucl. Phys.*

[5] Z. Trznadel, M. Kicińska-Habior, M. Kelly, J.P.S. van Schagen, K.A. Snover, to be published.

[6] J.J. Gaardhoje, *Nuclear structure at high excitation energy studied with giant resonances, Niels Bohr Institute, University of Copenhagen*, 1992.

[7] D. Brink, Ph. D. Thesis, Oxford University, Oxford 1955.

[8] M. Kicińska-Habior, K.A. Snover, C.A. Gossett, J.A. Behr, G. Feldman, H.K. Glatzel, J.H. Gundlach, E.F. Garman, *Phys. Rev.* **C36**, 612 (1987).

[9] Y. Alhassid, B. Bush, *Nucl. Phys.* **A514**, 434 (1990); **A531**, 1 (1991).

[10] D. Kusnezov, Y. Alhassid, K.A. Snover, *Proceedings of the Topical Conference on Giant Resonances, Varenna, May 11-16, 1998*, to be published in *Nucl. Phys.*

[11] Y. Alhassid, *Nucl. Phys.* **A569**, 37c (1994).

[12] J.H. Gundlach, K.A. Snover, J.A. Behr, C.A. Gossett, M. Kicińska-Habior, K.T. Lesko, *Phys. Rev. Lett.* **65**, 2523 (1990).

[13] Y. Alhassid, B. Bush, *Phys. Rev. Lett.* **65**, 2527 (1990).

[14] M. Kicińska-Habior, K.A. Snover, J.A. Behr, C.A. Gossett, J.A. Behr, Y. Alhassid, N. Whelan, *Phys. Lett.* **B308**, 225 (1993).

[15] Z.M. Drebi, K.A. Snover, A.W. Charlop, M.S. Kaplan, D.P. Wells, D. Ye, Y. Alhassid, *Phys. Rev.* **C52**, 578 (1995).

[16] A. Maj. M. Kicińska-Habior, J. Kownacki, W. Królas, J. Styczeń, J.J. Gaardhoje, T. Tveter, Z. Żelazny, M. Mattiuzzi, F. Camera, A. Bracco, B. Millon, Poster contribution on Gull Lake Nuclear Physics Conference on Giant Resonances, Gull Lake, 1993.

[17] J Hadermann, A.C. Rester, *Nucl. Phys.* **A231**, 120 (1974).

[18] P.H. Stelson, L. Grodzins, *Nuclear Data Tables* **1**, 21 (1965).

[19] P.Carlos *et al.*, *Nucl. Phys.* **A258**, 365 (1976); B.L. Berman, S.C. Fultz, *Rev. Mod. Phys.* **47**, 713 (1975).

[20] D.J. Parker, J. Asher, T.W. Conlon, I. Naqib, *Phys.Rev.* **C30**, 143 (1984).

[21] H. Ikezoe *et al.*, *Nucl. Phys.* **A444**, 349 (1985) and **A462**, 150 (1987).

[22] E. Gadioli *et al.*, *Phys. Lett.* **B394**, 29 (1997) and references therein.

[23] M.P. Kelly, J.F. Liang, A.A. Sonzogni, K.A. Snover, J.P.S. van Schagen, J.P. Lestone, *Phys. Rev.* **C56**, 3201 (1997).

[24] R. Vandenbosch, Fermi jet code, private communication.

[25] W. Cassing, V. Metag, U. Mosel, K. Niita, *Phys. Rep.* **188**, 363 (1990); also G. Wolf, BUU code, private communication.

[26] Y. Shutz *et al.*, *Nucl. Phys.* **A622**, 404 (1997).

[27] M. Kicińska-Habior, Z. Trznadel, K.A. Snover, A. Maj, M. Kelly, *Acta Phys. Pol.* **B28**, 189 (1997).